Co-published by
Institute of Fluid-Flow Machinery
Polish Academy of Sciences
Committee on Thermodynamics and Combustion
Polish Academy of Sciences

http://www.imp.gda.pl/archives-of-thermodynamics/

Complexity of two-phase flow dynamics using the recurrence and high speed video analysis

Romuald Mosdorf[a*], Gabriela Rafałko[a], Iwona Zaborowska[a], Paweł Dzienis[a], Hubert Grzybowski[a]

[a]Bialystok University of Technology, Faculty of Mechanical Engineering, Wiejska 45C, Bialystok 15-351, Poland
*Corresponding author email: r.mosdorf@pb.edu.pl

Received: 20.12.2023; revised: 15.03.2024; accepted: 15.04.2024

Abstract

During flow boiling in a system with small (mini/micro) channels, several instabilities may occur at the same time, which overlap each other – such a phenomenon complicates the analysis of boiling dynamics. The above mentioned processes cause that the fluctuation of recorded signals occur on various time scales. Although many criteria for the stability of two-phase flows are available, their practical application is limited (they need many recorded parameter of two phase flow). Methods which we are looking for should allow flow pattern identification based on a small number (or single) recorded signals. The paper presents a new approach to the recurrence plot method combined with Principal Component Analysis and Self-Organizing Map analysis. The single signal of pressure drop oscillations has been analyzed and used for flow pattern identification. New method of correlation analysis of flow patterns on video frames has been presented and used for flow pattern identification. The obtained results show that pressure drop oscillations and high speed video contain enough information about flow pattern for flow pattern identification.

Keywords: Instabilities; Two-phase flow; Recurrence analysis; Image analysis

Vol. 45(2024), No. 2, 73–81; doi: 10.24425/ather.2024.150853

Cite this manuscript as: Mosdorf, R., Rafałko, G., Zaborowska, I., Dzienis, P., & Grzybowski, H. (2024). Complexity of two-phase flow dynamics using the recurrence and high speed video analysis. *Archives of Thermodynamics*, 45(2), 73−81.

1. Introduction

Flow instability in the heated small (mini/micro) channel develops for high heat flux, which are the main factor determining the two-phase flow patterns in channels. The flow instabilities are related to the following processes: phase changes, heat flow, liquid and vapor flow as well as processes occurring in the heat exchanger's supply system with liquid and heat. With high heat flux supplied to the system, a small deviation from equilibrium leads to an exponential increase in the phase distribution [1]. Instabilities in two-phase flows accompanying boiling in small channels cause oscillations in the pressure drop, liquid and vapor flow rates, and channel wall temperatures.

Instabilities have been studied by Kennedy et al. [2], Kandlikar [3,4], Qu and Mudawar [5], Brutin et al. [6], Hetsroni et al. [7], and Bergles et al. [8], Tadrist [9], found that several types of instabilities observed in small channels are similar to those found in conventional channels. These include: Ledinegg instability, pressure drop oscillations and instability caused by changes in the mass flow density. During the experimental studies described in [10,11], oscillations in the pressure drop and

Nomenclature

DET − RQA coefficient, %
G − water flow rate, kg/(m^{2}s)
I − light intensity, scale from 0 to 255
k − percentage of the energy of light falling on the surface that was reflected
L − length, samples
L_{max} − RQA coefficient, samples
m − space dimensional
p − probability
P − histogram of probability, pressure, kPa
R − correlation coefficient
RPDE − RQA coefficient (entropy of points on diagonal lines)
S − $R_{max} - R_{avg}$
SD − standard deviation
T^1 − vertical distance in RP, samples
T^2 − vertical distance in RP, samples
V − volume, cm^3
V_v − coefficient
x − coordinate
Y − pixel brightness
z − channel number
|| || − norm

Greek symbols

α − angle between the vector normal to the surface and the direction of the observer, rad
$\Delta\alpha$ − the transparent diaphragm
$\Delta\beta$ − roughness of the channel bottom
$\Delta\delta$ − roughness of the mirror
ε − diameter of the sphere inside which the distance of two points is measured, samples
Θ − Heaviside step function
τ − delay time, samples

Subscripts and Superscripts

avg − average value
a − ambient light intensity
d − light source intensity
max − maximum
k − frame number

Abbreviations and Acronyms

PCA − Principal Component Analysis
RP − Recurrence Plot
SOM − Self-Organizing Map
RQA − Recurrence Quantification Analysis

temperature of the channel wall were noticed and videos were recorded showing periodic reverse flow in mini channels. This vapor flow heading into the inlet chamber is caused by the operation of the exchanger at critical values of the heat flux, which leads to mixing of the steam with the incoming subcooled liquid. In mini-channel systems, the influence of the channel wall temperature on heat transfer is much greater than in conventional systems. In channels with much smaller hydraulic diameter than the channel length, surface tension has a significant impact on the flow dynamics and stability of the system [12]. Fogg and Goodson in [13] investigated the influence of acoustic waves generated by rapidly nucleating bubbles during boiling in the flow in microchannels. It has also been shown that the negative pressure created by propagating pressure pulses can cause other bubbles to grow at lower channel wall temperatures.

The most commonly used classification, introduced by Bouré et al. [14], divides the instabilities of two-phase flow into static and dynamic. Static instabilities are considered to be momentary disturbances in which new operating conditions of the system tend to asymptotically change the state of the system - such a process is usually accompanied by high-frequency oscillations of pressure and temperature. On the other hand, dynamic instabilities are those in which a system cannot achieve a new equilibrium state, but only oscillates around a new equilibrium state. During dynamic instability, the system constantly changes its state between various unstable states - such a process is also accompanied by high-frequency oscillations of pressure and temperature. The occurrence of a number of instabilities causes the heat and mass transfer process in small channels to be non-stationary, therefore the analysis of boiling requires the use of methods that allow to characterize the non-stationary nature of the system. An important issue in the study of the boiling process in small channels is the identification of two-phase flow patterns in unsteady heat and mass transfer processes. Knowledge about the nature of non-stationary processes will allow the creation of more accurate models predicting heat and mass transfer in mini- and micro-channel systems.

Although many criteria for the stability of two-phase flows are available, their practical application for the analysis of heat transfer in real systems is limited [15]. This is because in real systems it is difficult to control all the flow parameters on the basis of which the nature of the two-phase flow is determined. Therefore, methods which we are looking for should allow flow identification based on a small number (or single) of recorded signals. In work [15] pressure drop oscillations and their impact on heat flux transferred through the exchanger were studied. It was shown that the time-averaged surface temperature and critical heat flux were insensitive to the occurrence of flow instability. Flow patterns identification was possible by taking into account high-frequency pressure oscillations and high-speed visualization.

In the paper [16] a method for indirect recognition of flow patterns was proposed, based on time-frequency analysis and neural networks. In order to examine flow patterns in a narrow rectangular channel, a pressure signal was used. The work [17] classified and summarized various methods of suppressing the instability of two-phase flows. The authors of the work concluded that more investigations should be done to identify instability under different operating conditions in different microchannel systems to avoid and suppress instability. In the paper [18], the authors showed that the use of machine learning becomes effective when the algorithms take into account the physical aspects of processes. Such solutions allow for the analysis of transition areas between boiling regimes.

When examining boiling in two-phase flow in channels on a mini- and micro-scale, a number of experimental data are rec-

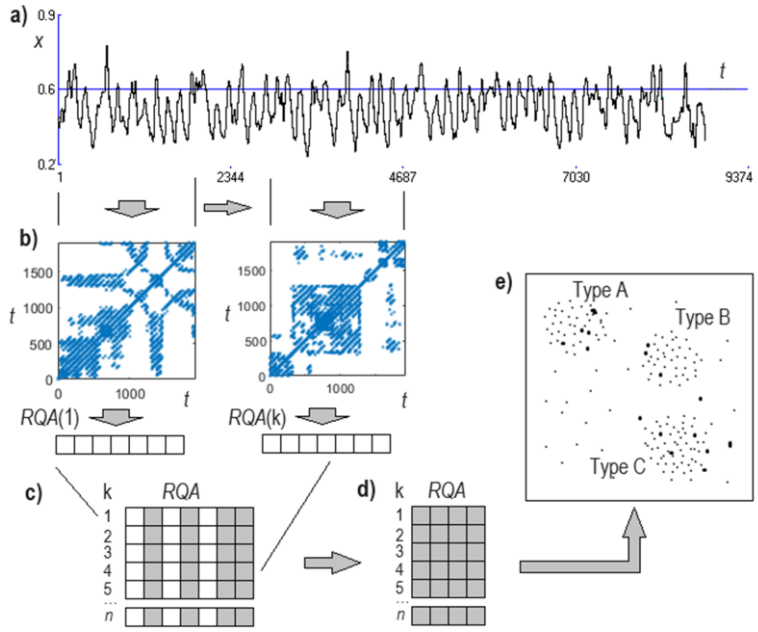

Fig. 1. Scheme of the algorithm for identifying two-phase flow patterns based on pressure fluctuations: a) an example of registered signal, b) the results of RQA analysis, c) a matrix of RQA coefficients determined in subsequent time intervals, d) selection of RQA coefficients, e) PCA or SOM analysis.

orded which contain information about the nature of the phenomenon. Experimental data includes, among others, measurement of pressure changes, liquid temperature changes, channel wall temperature changes and video data recorded by high-speed cameras. Pressure oscillations occurring in two-phase flow contain a lot of noise resulting from the changes in the two-phase flow patterns, therefore, they are difficult to analyze. At the same time, pressure oscillations have an irregular, chaotic character. One of the basic features of a chaotic systems is recurrence, which can be used in the analysis of pressure oscillations.

In this paper the recurrent patterns in the pressure oscillation signal are applied to identify changes in two-phase flow structures. Selected methods for analyzing the dynamics of two-phase flow patterns based on video analysis are also presented.

2. Application of recurrent analysis to study pressure fluctuations

2.1. Algorithm

In Fig. 1a, a diagram of the algorithm for identifying two-phase flow patterns based on pressure fluctuations is shown [19]. Figure 1a shows an example of the registered signal - pressure fluctuations. Figure 1b schematically shows two stages of RQA analysis. In the first stage, the attractor is reconstructed in the multidimensional phase space. Then recurrence plots are created – this process is schematically shown in Fig. 1b. A recurrence plot is a two-dimensional (square) matrix containing zeros and ones. The matrix dimension defines the number of analyzed samples (schematically marked by the black lines in Fig. 1a). RQA analysis involves determining a series of coefficients characterizing the arrangement of ones in the matrix. In the considered method the RQA coefficients are determined for subsequent time intervals [19]. The result of calculation of the RQA coefficient is shown schematically in Fig. 1c as the matrix. A statistical analysis of the changes in the values of RQA coefficients allows the selection of coefficients that best describe the diversity of the two phase flow pattern changes. This analysis creates the matrix shown in Fig. 1d. The visualization of the data in the matrix shown in Fig. 1e can be performed using PCA or neural networks (SOM) methods.

From the formal point of view the recurrence plot is defined as follows [20]:

$$RP_{i,j} = \Theta\left(\varepsilon - \left\|x_i - x_j\right\|\right), \qquad i,j = 1,\dots,N, \tag{1}$$

where $\Theta(\cdot)$ – Heaviside step function, ε – diameter of the sphere inside which the distance of two points is measured, $\|\ \|$ – norm in m-dimensional space.

The *DET* coefficient determines the percentage of recurrence states occurring on diagonal lines to all recurrence states of the system [20]:

$$DET = \frac{\sum_{l=l_{min}}^{N} lP(l)}{\sum_{l=1}^{N} lP(l)}, \tag{2}$$

where $P(l) = P(\varepsilon, l)$ is the histogram of diagonal lines of length l in the neighborhood of ε.

The L coefficient determines the average length of the diagonal lines in a recurrence plot. The L coefficient is described by the following relation [20]:

$$L = \frac{\sum_{l=l_{min}}^{N} lP(l)}{\sum_{l=l_{min}}^{N} P(l)}. \tag{3}$$

The L_{max} coefficient determines the maximum length of diagonal lines.

The *RPDE* coefficient is a measure of the entropy of points on diagonal lines. The *RPDE* coefficient is described by the following relation [20]:

$$RPDE = -\sum_{l=lmin}^{N} p(l)\ln p(l), \quad (4)$$

where $p(l)$ is the probability of finding a diagonal line of length l: $p(l) = \frac{P^{\varepsilon}(l)}{\sum_{l=lmin}^{N} P^{\varepsilon}(l)}$.

Entropy is a measure of uncertainty – an increase in the *RPDE* coefficient means that the system becomes more chaotic.

Gao [21] defines the recurrence time of the first type T^1 and the second time T^2. The recurrence time is calculated as the distance between points belonging to the vertical lines in *RP*. In the case of recurrence time of the first type T^1, all points of *RP* are considered. Such value of T^1 depends on the trajectory density and value of ε. In case of recurrence time of the second type T^2 the vertical distances between the pairs "white" pixel/"black" pixel in the columns are measured [22]. Then, in this case for the periodic motion, T^2 accurately estimates the period of the motion.

2.2. Application

The paper presents the results of the method (Fig. 1) application for analyzing pressure fluctuations in a single mini-channel and in an exchanger consisting of many parallel mini-channels [19,23]. Figure 2a shows a diagram of the measurement stand and Fig. 2b shows example pressure drop fluctuations. The pressure fluctuation amplitudes shown in Fig. 2b increase when vapor bubbles appear in the heated channel, blocking the flow (at the beginning of the cycle the channel is filled with water). When the slug flow begins, the amplitude of pressure fluctuations reaches its maximum values (90 seconds after the beginning of the cycle).

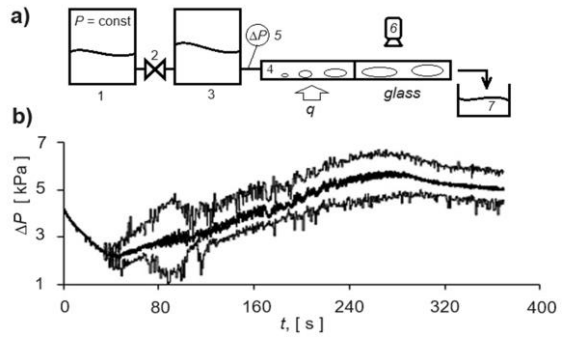

Fig. 2. a) the scheme of the experimental stand: single-channel exchanger, 1 – supply tank; 2 – ball valve; 3 – compressible volume; 4 – heat exchanger; 5 – pressure sensor, 6 – Phantom camera, 7 – output tank; b) pressure drop fluctuations, the chart showing the minimum, maximum and average value of water pressure oscillations at the inlet to the channel; channel diameter – 1 mm, water flow rate, G = 159 kg/(m^{2}s), electric power 57.2 W [19].

The moving window in the windowed RQA analysis contained 5000 samples of pressure oscillations (5s), and the window shift was equal to 1000 samples of pressure oscillations (1s) – 181 windows were analyzed. The RQA coefficient values were calculated using the CRP package [23] in MATLAB. The length of the time window in the RQA analysis was determined by pressure oscillations caused by flowing long slug, which generate pressure changes that occur at low frequency. The assumed interval of 5 s corresponds to the flow of approximately 5 long slugs. In the RQA window analysis, the parameters of the immersion dimension (m), delay time (τ) and threshold distance (ε) were determined separately for each window. The dimension m was estimated using the false nearest neighbours method [23]. The value of τ was selected using the mutual information function [24], while the value of ε was defined as 10% of the maximum attractor diameter. Figure 3 shows the changes in coefficients (*DET*, 1/*L*, T^2, 1/*RPDE*). The values of these coefficients were used to build the SOM map shown in Fig. 4.

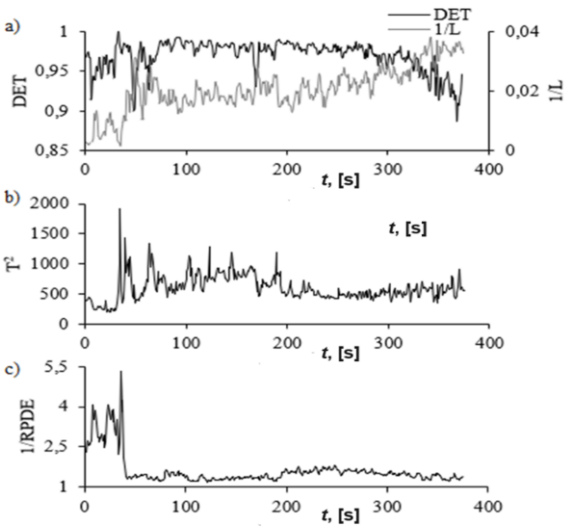

Fig. 3. The changes in the RQA coefficients obtained for water pressure oscillations at the inlet to the mini-channel at G = 159 kg/(m^{2}s), electric power equal to 57.2 W: a) *DET*, 1/*L*, b) T^2, c) 1/*RPDE*; calculations were performed using the RP package [23] in Matlab.

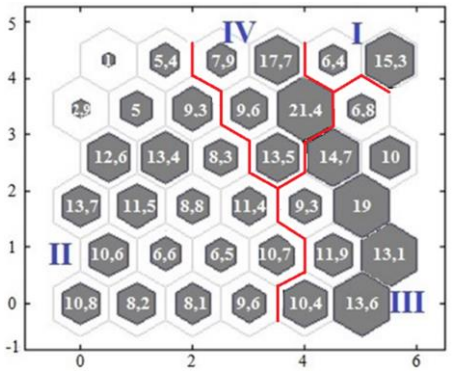

Fig. 4. Average hit histograms obtained from RQA coefficients calculated for inlet water pressure oscillations at: G = 159 kg/(m^{2}s), electric power equal to 57.2 W [25].

The changes in the *DET* coefficient presented in Fig. 3a show that changes in the character of pressure fluctuations occur rapidly in the initial phase of boiling - in bubble flow and in the initial phase of slug flow. Such behaviour appear also at the end of the cycle - when the increasing average pressure value leads to boiling disappearance. The average length of the diagonal line shown in Fig. 3a determines the average duration of a given flow

pattern in the channel – it is the smallest at the end of the cycle (boiling disappearance) and the largest at the beginning of the cycle when the boiling begins. Fluctuations in the T^2 coefficient reflect changes in the characteristic frequencies of pressure fluctuations. The nature of the changes is most rapid in the initial phase of boiling and in slug flow. The entropy values shown in Fig. 3c show the chaotic character of pressure fluctuations during the boiling in the channel.

In Fig. 4, four local maxima can be distinguished, which identify four different two-phase flow patterns.

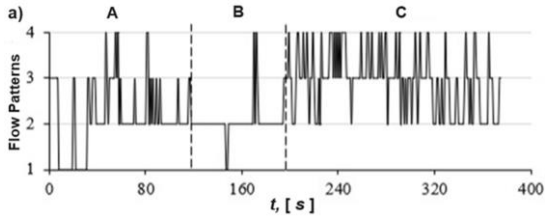

	Two-phase flow patterns			
	1	2	3	4
A	19%	52%	26%	3%
B	2%	89%	6%	3%
C	0%	27%	54%	19%

Fig. 5. Results of the RQA and SOM analysis obtained for inlet pressure, G = 159 kg/(m^{2}s) and electric power equal to 57.2 W: a) distinguished two-phase flow patterns (vertical axis) - result of training the SOM network (number of local maximum) and they accuracy in time; b) the percentage of the two-phase flow patterns present in the boiling flow. 1 – water flow with small bubbles, 2 – bubble flow, 3 – slug flow, 4 – long slug flow [25].

The analysis of changes in time these patterns, performed on the basis of data collected in the SOM algorithm, allows the identification of the flow patterns, these were: 1 – water flow with small bubbles, 2 – bubble flow, 3 – slug flow, 4 – long slug flow. The ranges of occurrence of flow patterns are shown in Fig. 5.The result of SOM algorithm (distinguished two-phase flow patterns - vertical axis and they accuracy in time are presented in Fig. 5a. The percentage of the two-phase flow patterns presents in the boiling flow is presented in Fig. 5b.

3. Analysis of the dynamics of phase change based on videos

3.1. Algorithm

The validation of the results presented in the previous chapter were performed using the recorded videos of two-phase flow. The videos contain information about processes that are not visible in the pressure fluctuations. Therefore, selected methods for analyzing the dynamics of two-phase flow patterns based on image (video) analysis are presented below. The analysis of characteristic flow features was carried out on the basis of pixel brightness changes. The similarity and complexity of phase distribution were analyzed.

The presented method for examining the similarity of the phase distribution uses the Pearson correlation coefficient. The initial step of the analysis is to divide the recorded videos into frames. The example of the frames set is schematically shown in Fig. 6a.

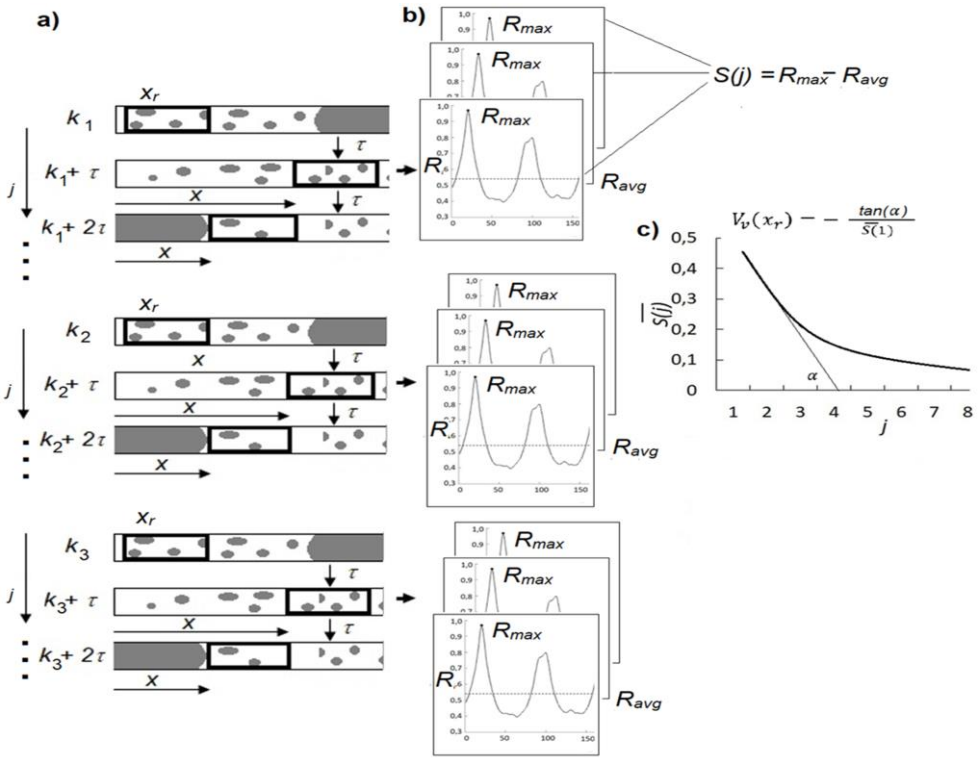

Fig. 6. Two-phase flow video analysis scheme: a) subsequent video frames, reference frames (k) and reference gates (x_r – position of the reference gate), test frames ($k + \tau$ – test frame number), τ – time between subsequent test frames, x – position of the moving gate; arrows indicate the flow direction; b) correlation between the reference gate and the test gates; c) plot of the average values ($R_{max} - R_{avg}$) for subsequent test gates [25].

In the set of frames (Fig. 6a), reference frames (k) and reference gates (x_r - position of the reference gate) are defined. On test frames $k + \tau$, test gates are moved, the position of which is denoted with x. In this way, for each reference gate, a set of graphs is created which describe correlation between reference gate and test gates moving on subsequent test frames. A set of graphs obtained in this way is schematically shown in Fig. 6b. The following value is determined for each graph:

$$S(j) = R_{max} - R_{avg} \tag{5}$$

The $S(j)$ is averaged for subsequent (all) test gates, finally the graph shown in Fig. 6.c is created. The graph is used to determine the value of the V_v coefficient in accordance with the following relation:

$$V_v = -\frac{\tan(\propto)}{\bar{S}(1)}. \tag{6}$$

The algorithm was used to identify flow patterns [25,26]. The analysis of the flow of a mixture of water, glycerin and air showed that the V_v coefficient reaches the lowest values for slug flows and the highest in the case of mini-bubble flows. The slug flow is characterized by smaller changes in phase distribution than mini-bubble flow, which results in a lower value of the V_v coefficient. The obtained result confirms that the value of the V_v coefficient characterizing the "speed" of phase distribution changes in channel.

3.2. Application

The algorithm presented in the previous chapter (Fig. 6) was used to determine the position of the boiling front in an exchanger with parallel mini channels [25,27]. It was assumed that the change in phase distribution occurs most rapidly in the place where the boiling front is formed in parallel microchannels. Therefore in the previous algorithm (Fig. 6), additionally, the movement of the reference gate position was taken into account. Finally, in order to identify the channel fragments with the most rapid phase distribution changes, the position of the reference gate was searched for at which the V_v coefficient reaches its maximum value.

The scheme of the experimental stand is shown in Fig. 7.

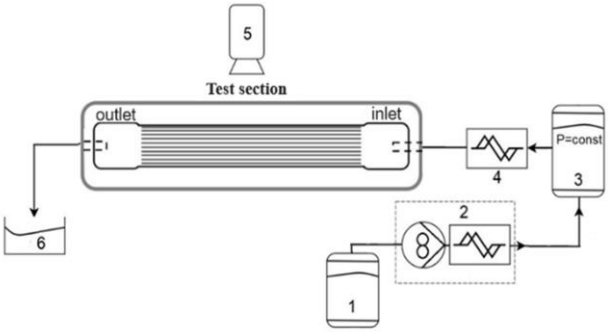

Fig. 7. Experimental stand with microchannels: 1 - feed tank with distilled water, 2 – gear pump with flowmeter (Bronkhorst Cori-Tech M13 with pump), 3 – compressible volume (V = 222.8 cm^3), 4 – flowmeter (Bronkhorst mini CORI-FLOW M13, accuracy ± 0.2% of flow rate), 5 – high-speed camera (Phantom v1610), 6 – outlet tank.

The working medium (distilled water) - see Fig. 7, was supplied from the supply tank (1) by a gear pump (2) connected to a flowmeter (Bronkhorst Cori-Tech M13 with pump, accuracy 2% of the measured value) to the compressible volume (3). The flow rate of water supplied to the inlet space was monitored by a mass flow meter (4) (Bronkhorst Cori-Tech M13 based on the Coriolis measuring principle) installed between the compressible volume and the exchanger (microchannels exchanger consisting of 11 copper microchannels: depth × width × length = 0.13 × 0.25 × 32 mm). Pressure sensors (MPX50DP, range: 0−50 kPa, sensitivity: 1.2 mV/kPa, response time: 0.001 s, accuracy: 1.25 kPa) and thermocouples (type K, diameter 0.081 mm, accuracy: ± 0.8 K, response time: 0.025 s) were installed. After passing through the channels, the water headed to the outlet tank (6). The flow of the medium through the channels was recorded using a high-speed camera - Phantom v1610 (5) through a transparent plexiglass and a mirror. The heat flux supplied to the channels was measured by three thermocouples (type K, diameter 0.081 mm, accuracy: ± 0.8 K, response time: 0.025 s) located in a copper pin. Heat was supplied to the system using eight electric heaters with a maximum power of 50 W. During the experiment, the electrical power supplied to the system was constant, while the liquid flow rate varied. Two measurement data acquisition systems were used (DAQ Data Translation DT9804, Data Translation DT9805) and collected data at a frequency of 1 kHz.

3.3. Measurement error analysis

In this work, the analyzed physical quantity is the pixel brightness (Y) recorded by the Phantom v1610 camera. The level of pixel brightness recorded by the camera is a function of the light intensity reaching the camera lens , and is determined by the relationship [28]:

$$Y = I_a + I_d k \cos\alpha, \tag{7}$$

where: I_a – ambient light intensity, I_d – point light intensity of the light source, k – percentage of the energy of light falling on the surface that was reflected, α – angle between the vector normal to the surface and the direction of the observer.

To determine the absolute maximum uncertainty of pixel brightness resulting from the intensity of light reaching the camera (Y), the complete differential method was used. It was determined on the basis of the uncertainty of individual arguments: roughness of the transparent diaphragm ($\Delta\alpha$), roughness of the channel bottom ($\Delta\beta$) and roughness of the mirror ($\Delta\delta$):

$$Y = \cos\left(\left|\frac{\partial f(\alpha,\beta,\delta)}{\partial\alpha}\right|\Delta\alpha + \left|\frac{\partial f(\alpha,\beta,\delta)}{\partial\beta}\right|\Delta\beta + \left|\frac{\partial f(\delta\alpha,\beta,\delta)}{\partial\delta}\right|\Delta\delta\right). \tag{8}$$

The analysis of the roughness of the channel bottom surface was performed using a VHX-7000 optical microscope (Keyence) at x700 magnification. The pixel brightness error was ±0.13 on a scale from 0 to 255. This allows us to conclude that the proposed image analysis method has a small error.

Figure 8a shows the V_v coefficient obtained for single microchannel which is shown in Fig. 8b. The value of the V_v coefficient identifies the position of the reference gate (x_r) where the "speed" of phase distribution changes reach the maximum.

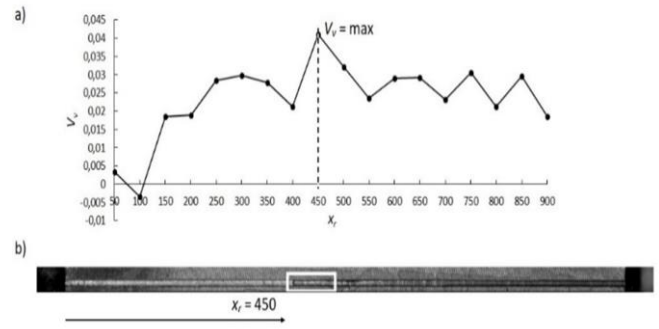

Fig. 8. Determining the channel fragments with the most rapid phase distribution changes: a) V_v coefficient as a function of the position of the reference gate (x_r – number of pixels); b) single frame of video with channel, the position of the maximum value of V_v coefficient was marked by a rectangle [25].

The location of the most rapid phase distribution changes determined for the entire exchanger is shown in Fig. 9. Figure 9 shows the positions of the reference gates (in the form of a point) in subsequent microchannels at which the V_v coefficient reaches its maximum. Fig. 9b shows an example video frame with the marked positions of the reference gates indicating the location of the most significant phase distribution changes.

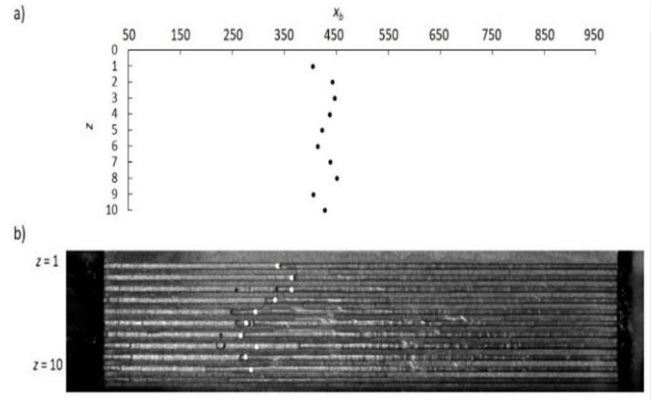

Fig. 9. The location of the most rapid phase distribution changes: a) chart showing the location of the most rapid phase distribution changes (black points); b) an example video frame with the marked positions of the reference gates indicating the location of the most significant phase distribution changes, (x_b – number of pixels from the inlet, z – channel number) [25].

An analysis of the repeatability of the results obtained using the phase distribution similarity method for assessing the dynamics of phase change was carried out. The aim of the repeatability analysis was to determine the size of the dispersion of the boiling front positions in the considered flow fragments. The multiple calculations of the reference gate positions at which the V_v coefficient reached its maximum were carried out for various fragments of recorded videos. The results of calculation for 10 microchannels have been shown in Table 1.

Table 1. The results of the repeatability analysis. z − microchannel number, 1−6 − considered fragments of the film, x_r − position of the boiling front, *avr* − average value of x_r in each microchannel, *SD* – standard deviation of the position of x_r, [25].

z (-)	Considered fragments of the film				*avr* (mm)	*SD* (mm)
	1	2	...	6		
	x_b (mm)	x_b (mm)		x_b (mm)		
1	10.00	11.25		7.50	9.58	1.91
2	8.75	12.50		7.50	9.58	2.60
3	8.75	8.75		11.25	9.58	1.44
4	8.75	6.25		8.75	7.92	1.44
5	10.00	7.50		8.75	8.75	1.25
6	7.50	10.00		8.75	8.75	1.25
7	10.00	10.00		7.50	9.17	1.44
8	7.50	6.25		6.25	6.67	0.72
9	6.25	8.75		10.00	8.33	1.91
10	10.00	7.50		11.25	9.58	1.91

The obtained results show that the proposed analysis method is repeatable and determines the location of the boiling front with an error equal about 20%.

4. Conclusions

The research carried out is consistent with the current research direction in published works which involves the identification of flow patterns based on high-frequency changes in single parameters of two-phase flows. The current work analyzed high-frequency pressure oscillations and high-frequency changes in pixel brightness in high-speed video frames. The paper presents a new approach to flow boiling pattern identification using recurrence plot method combined with PCA and SOM analysis. The new method of correlation analysis of flow patterns on video frames has been presented and used for flow pattern identification.

The obtained results show that pressure drop oscillations and high speed video contain enough information about flow pattern for flow pattern identification. It has been shown that the methods of analyzing boiling pressure fluctuations in small channels using recurrence analysis enable the identification of two-phase flow patterns in boiling. Moreover, the information contained in the pixels brightness changes in the videos directly recorded during two-phase flows in small channels allows identifying flow patterns and studying processes occurring in boiling.

The use of the methods proposed in this paper to identify flow patterns based on selected measurement data is effective, but their application to other measurement data requires a preliminary analysis of the measurement data. An important parameter is the sampling frequency - it cannot be too high because then the signal will be noisy - which will prevent the extraction of important flow features. In this case, signal filtering can be used, but such manipulation of measurement data may affect the result of identifying flow patterns. The sampling frequency cannot be too low because the signal will not contain enough information about important characteristics of the flow patterns. In

the case under consideration in the paper, both sampling frequency of pressure changes and the speed of film frames registration were sufficient to identify the flow of individual bubble, increasing the water flow rate would require increasing the sampling frequency. Research on selecting an appropriate sampling frequency should be continued for different cases.

The new data analysis methods presented in the paper was tested on data collected in experiments performed by the authors of the work. During our measurements the appropriate data recording parameters were set. The analysis methods proposed in this work were also applied to other types of measurement data in order to determine their suitability for identifying selected features of time series. In these cases medical data [30], tribological data [31] and the process of air bubbles departure from nozzles [29] were analyzed. The obtained results confirm the high effectiveness of the analysis methods presented in the paper.

Acknowledgements

The research was funded by the National Science Center grant UMO-2017/27/B/ST8/02905.

References

[1] Ruspini, L.C., Marcel, C.P., & Clausse, A. (2014). Two-Phase Flow Instabilities: A Review. *International Journal of Heat and Mass Transfer*, 71, 521–548. doi: 10.1016/j.ijheatmasstransfer. 2013.12.047

[2] Kennedy, J.E., Roach, G.M., Dowling, M.F., Abdel-Khalik, S.I., Ghiaasiaan, S.M., Jeter, S.M., & Quershi, Z.H. (2000). The Onset of Flow Instability in Uniformly Heated Horizontal Microchannels. *J. Heat Transfer*, 122, 118–125. doi: 10.1115/1.521442

[3] Kandlikar, S.G. (2002). Fundamental Issues Related to Flow Boiling in Mini channels and Microchannels. *Experimental Thermal and Fluid Science*, 26, 389–407. doi: 10.1016/s0894-1777(02) 00150-4

[4] Kandlikar, S., Steinke, M., Tian, S., & Campbell, L. (2001). High-Speed Photographic Observation of Flow Boiling of Water in Parallel Mini-Channels. *Proceedings of NHTC'01 35th National Heat Transfer Conference*, Anaheim, California

[5] Qu, W., & Mudawar, I. (2003). Measurement and Prediction of Pressure Drop in Two-Phase Micro-Channel Heat Sinks. *International Journal of Heat and Mass Transfer*, 46, 2737–2753. doi: 10.1016/S0017-9310 (03)00044-9

[6] Brutin, D., Topin, F., & Tadrist, L. (2003). Experimental Study of Unsteady Convective Boiling in Heated Minichannels. *J. Heat Transfer*, 46, 2957–2965. doi:10.1016/S0017-9310(03)00093-0

[7] Hetsroni, G., Mosyak, A., Segal, Z., & Pogrebnyak, E. (2003). Two-Phase Flow Patterns in Parallel Micro-Channels. International Journal of Multiphase Flow, 29, 341–360. doi: 10.1016/ S0301-9322(03)00002-8

[8] Bergles, A.E., Lienhard V. J.H., Kendall, G.E., & Griffith, P. (2003). Boiling and Evaporation in Small Diameter Channels. *Heat Transfer Engineering*, 24, 18–40. doi: 10.1080/01457630304041

[9] Tadrist, L. (2007). Review on Two-Phase Flow Instabilities in Narrow Spaces. *International Journal of Heat and Fluid Flow*, 28, 54−62. doi: 10.1016/j.ijheatfluidflow.2006.06.004

[10] Grzybowski, H., & Mosdorf, R. (2018). Dynamics of Pressure Drop Oscillations during Flow Boiling inside Minichannel. *International Communications in Heat and Mass Transfer*, 95, 25–32. doi:10.1016/j.icheatmasstransfer.2018.03.025

[11] Rafałko, G., Zaborowska, I., Grzybowski, H., & Mosdorf, R. (2020). Boiling Synchronization in Two Parallel Mini channels - Image Analysis. *Energies*, 13, 1409. doi: 10.3390/en13061409

[12] Yarin, L.P., Mosyak, A., & Hetsroni, G. (2009) Fluid Flow, Heat Transfer and Boiling in Micro-Channels; *Heat and Mass Transfer*; Springer-Verlag: Berlin Heidelberg, doi:10.1007/978-3-540-78755-6

[13] Fogg, D., & Goodson, K. (2009). Bubble-Induced Water Hammer and Cavitation in Microchannel Flow Boiling. *J. Heat Transfer*, 131, 1–12. doi:10.1115/1.3216381

[14] Boure, J.A., Bergles, A.E., & Tong, L.S. (1973). Review of Two-Phase Flow Instability. *Nuclear Engineering and Design*, 25, 165−192. doi: 10.1016/0029-5493 (73)90043-5

[15] Clark, M.D., Weibel, J.A., & Garimella S.V. (2023), Impact of pressure drop oscillations and parallel channel instabilities on microchannel flow boiling and critical heat flux. *International Journal of Multiphase Flow*, 161, 104380. doi: 10.1016/j.ijmultiphaseflow.2023.104380

[16] Chu, A.W., Liu, B.Y., Pan, C.L., Zhu, D.H., & Yang, E.X. (2022). Identification of boiling flow pattern in narrow rectangular channel based on TFA-CNN combined method. *Flow Measurement and Instrumentation*, 83, 102086. doi: 10.1016/j.flowmeasinst.2021. 102086

[17] Wang, B., Hu, T., He, Y., Rodionov, N., & Zhu, J. (2022). Dynamic instabilities of flow boiling in micro-channels: A review. *Applied Thermal Engineering*, 214, 118773. doi: 10.1016/j.applthermaleng .2022.118773

[18] Zhu, L., Ooi, Z.J., Zhang, T., Brooks, C.S., & Pan, L. (2023). Identification of flow regimes in boiling flow with clustering algorithms: An interpretable machine-learning perspective. *Applied Thermal Engineering*, 228, 120493. doi: 10.1016 /j.applthermaleng.2023.120493

[19] Zaborowska, I. (2023). *Experimental studies and numerical identification of the dynamics of two-phase flow patterns in boiling in mini- and micro-channels*. PhD thesis, Bialystok University of Technology.

[20] Zbilut, J.P., & Webber, C.L. (1992). Embeddings and Delays as Derived from Quantification of Recurrence Plots. *Physical Letters A*, 171, 199–203. doi: 10.1016/0375-96 01(92)90426-M

[21] Gao, Z.-K., Jin, N.-D., & Wang, W.-X. (2014). *Nonlinear analysis of gas-water/oil-water two-phase flow complex networks*. Springer: Berlin, Heidelberg. doi: 10.1007/978-3-642-38373-1_1

[22] Gao, Z.-K., Zhang, X.-W., Jin, N.-D., Donner, R.V., Marwan, N., & Kurths, J. (2013). Recurrence Networks from Multivariate Signals for Uncovering Dynamic Transitions of Horizontal Oil-Water Stratified Flows. *Europhysics Letters*, 103(5), 50004. doi: 10.1209/ 0295-5075/103/50004

[23] Zaborowska, I., Grzybowski, H., Rafałko, G., & Mosdorf, R. (2021). Boiling dynamics in parallel minichannel system with different inlet solutions, *International Journal of Heat and Mass Transfer*, 165, 1–10. doi: 10.1016/j.ijheatmasstransfer.2020. 120655

[24] Marwan, N. *Cross Recurrence Plot Toolbox for MATLAB®, Ver. 5.22*. http://Tocsy.Pik-Potsdam.de/ CRPtoolbox/ [accessed 08 Feb. 2024].

[25] Rafałko, G. (2023). *Application of image analysis to identify and investigate the dynamics of two-phase flow patterns.* PhD thesis, Bialystok University of Technology.

[26] Rafałko, G., Mosdorf, R., & Górski, G. (2020). Two-phase flow pattern identification in mini channels using image correlation analysis, *International Communications in Heat and Mass Transfer*, 113, 1–9. doi: j.icheatmasstransfer.2020.104508

[27] Rafałko, G., Grzybowski, H., & Mosdorf, R. (2022). An image analysis method of liquid phase distribution during boiling in parallel mini channels, *International Communications in Heat and Mass Transfer*, 139, 1–10. doi: 10.1016/j.icheatmasstransfer.2022.106453

[28] Lu, R. (2017). Light Scattering Technology for Food Property, *Quality and Safety Assessment*. CRC Press. doi: 10.1201/b20220

[29] Dzienis, P., Zaborowska, I., & Mosdorf, R. (2022). JRP analysis of synchronization loss between signals recording during bubble departures. *Nonlinear Dynamics*, 108, 433–444. doi: 10.1007/s11071-022-07217-9

[30] Gruszczyńska, I., Mosdorf, R., Sobaniec, P., Żochowska-Sobaniec, M., & Borowska, M. (2019). Epilepsy identification based on EEG signal using RQA method, *Advances in Medical Sciences*, 64(1), 58–64. doi:10.1016/j.advms.2018.08.003

[31] Łępicka, M., Grądzka-Dahlke, M., Zaborowska, I., Górski, G., & Mosdorf, R. (2022). Recurrence analysis of coefficient of friction oscillations in DLC-coated and non-coated Ti6Al4V titanium alloy. *Tribology International*, 165, 107342. doi: 10.1016/j.triboint.2021. 107342